

Time Evolution of Density Fluctuation in Supercritical Region. I. Non-hydrogen-bonded Fluids Studied by Dynamic Light Scattering

Ken-ichi Saitow*

Department of Physics, Faculty of Science, Chiba University, Yayoi, Inage, Chiba 263-8522, Japan

Daisuke Kajiya and Keiko Nishikawa

Division of Diversity Science, Graduate School of Science and Technology, Chiba University, Yayoi, Inage, Chiba 263-8522, Japan

Received: August 2, 2004

The time evolution of the density fluctuation of molecules inhomogeneously dispersing in a mesoscopic volume is investigated by dynamic light scattering in several fluids in supercritical states. This study is the first time-domain investigation to compare the dynamics of density fluctuation among several fluids. The samples used are non-hydrogen-bonded fluids in the supercritical states: CHF_3 , C_2H_4 , CO_2 , and xenon. These four molecules have different properties but are of similar size. Under these conditions, the relationship between dynamic and static density inhomogeneities is studied by measuring the time correlation function of the density fluctuation. In all cases, this function is characterized by a single exponential function, decaying within a few microseconds. While the correlation times in the four fluids show noncoincidence, those values agree well with each other when scaled to a dimensionless parameter. From the results of this scaling based on the Kawasaki theory and Landau–Placzek theory, the relation between dynamics and static structures is analyzed, and the following four insights are obtained: (i) viscosity is the main contributor to the time evolution of density fluctuation; (ii) the principle of corresponding state is observed by the use of time-domain data; (iii) the Kawasaki theory and the Landau–Placzek theory are confirmed to be applicable to polar, nonpolar, and nondipolar fluids that have no hydrogen bonding, at temperatures relatively far from critical temperature; and (iv) the density fluctuation correlation length and the value of density fluctuation are estimated from the time-domain data and agree with the values from other experiments and calculations.

I. Introduction

The increasing use of supercritical fluids in a wide range of practical applications has motivated many recent attempts to understand the fundamental aspects of fluid structure. Although, for decades, the inhomogeneity of fluid structures around gas–liquid critical points was considered to be a result of density inhomogeneity, the supercritical fluid structure recently has been associated with efficiencies of extraction and chemical reaction.^{1–5} For example, the solubility, rate constant, and yield of the photochemical reaction, as well as the relaxation times of electronic, vibrational, and rotational transitions, each show an inflection, a minimum or a maximum around the density where the inhomogeneity is greatest. Thus, it is important to study supercritical fluids with regard to inhomogeneity, not only to increase our understanding of the natural sciences but also to improve efficiencies in the chemical industry.

From the point of view of experimental studies to investigate inhomogeneity, light scattering measurements have proven to be a good method in the condensed phase.^{6–8} The light scattering is characterized by two different schemes, i.e., elastic scattering and quasi-elastic scattering. In the former, the energy before and after scattering is conserved, and the momentum is transferred between the incident light and the medium. From

this elastic scheme, static structures in the condensed phases are measured from the intensity of Rayleigh scattering, as a function of the scattering vector, representing the magnitude of the transferred momentum. On the other hand, the quasi-elastic scattering scheme is ascribed to subtle energy transfer between the incident light and the medium. A Rayleigh linewidth in the frequency domain and a time correlation function in the time domain are given by spectral measurements and by dynamic light scattering (DLS) measurements, respectively. Thus, dynamic structures of fluids are characterized by these measurements and analyses.

Light scattering studies relating to supercritical fluids started in 1970 as research into the critical phenomena of the gas–liquid critical point.^{9–14} Although there have not been many studies on light scattering for supercritical fluid structures, the structures of several such fluids were reported by measuring the Rayleigh scattering intensity^{9–12} or the Rayleigh scattering spectrum.^{12–14} These studies were conducted in thermodynamic states along the critical isochore very near the gas–liquid critical temperature, i.e., $1.000005 \leq T_r = T/T_c \leq 1.001$. Several researchers investigated static structures of CO_2 , and correlation lengths were obtained using the Ornstein–Zernike–Fisher theory.^{9–11} As for dynamic structures, supercritical CO_2 ,¹³ xenon,¹³ and SF_6 ^{12–14} were investigated in the *frequency domain*. The Rayleigh linewidths of these fluids were measured, and decay rates of density fluctuation and transport coefficients were discussed using the Kawasaki theory^{15,16} and Landau–Placzek theory.¹⁷ Recently, dynamic structures have been investigated

* Author to whom correspondence should be addressed. Present address: Material Science Center, Natural Science Center for Basic Research and Development, Hiroshima University, 1-3-1 Kagamiyama, Higashi Hiroshima 739-8526, Japan. Tel/fax: +81-82-424-7487. E-mail: saitow@hiroshima-u.ac.jp.

TABLE 1: Molecular Properties and Critical Constants

molecule	radius ^{a,b} (nm)	volume ^{a,b} ($\times 10^3$ nm ³)	structure	polarity ^c	T_c (K)	P_c (MPa)	ρ_c (g/cm ³)
Xe	0.216	42.2	spherical		289.73 ^g	5.84 ^g	1.1 ^g
CHF ₃	0.214	41.1	sym. top	1.65 D ^d	299.06 ^h	4.836 ^h	0.525 ^h
C ₂ H ₄	0.210	38.8	plane	-4 D Å (Q_{xx}) ^e	282.35 ⁱ	5.042 ⁱ	0.214 ⁱ
				2 D Å ($Q_{yy} = Q_{zz}$) ^e			
CO ₂	0.201	34.0	linear	-20 D Å (Q_{xx}) ^f	304.13 ^j	7.377 ^j	0.468 ^j
				-15 D Å ($Q_{yy} = Q_{zz}$) ^f			

^a Data taken from ref 23. ^b Each molecular radius and volume are given by the van der Waals radius and volume, respectively. Their values were measured by XRD measurements from ref 23. ^c Units of dipole moment (D) and quadrupole moments (D Å) in the table are debye and debye angstrom, respectively. The value of quadrupole moment is represented by a tensor element in each principal axis. ^d Data taken from ref 24. ^e Data taken from ref 25. ^f Data taken from ref 26. ^g Data taken from ref 27. ^h Data taken from ref 28. ⁱ Data taken from ref 29. ^j Data taken from ref 30.

by DLS in the *time domain* measurements, and the “critical slowing down” of diffusing molecules has been observed in a wider density range.^{18,19} From those results, a time-constant map of the “critical slowing down” was produced as a contour curve on phase diagrams,¹⁹ and the structures of the supercritical fluids observed by diffusive motion were discussed in relation to the local structures of the same fluid observed by vibrational and rotational motions.^{20–22}

In the present study, we investigate the time evolutions of molecules at the supercritical states of several fluids by measuring DLS. To the best of our knowledge, this study is the first time-domain investigation to compare the dynamics of density fluctuations among several fluids. The samples used here are non-hydrogen-bonded fluids in the supercritical state, i.e., CHF₃, C₂H₄, CO₂, and xenon. These four molecules have different properties, as listed in Table 1, but similar sizes. The present DLS experiments on these neat supercritical fluids were performed in a wide density range at temperatures relatively far from critical temperature, i.e., $T_r = 1.01–1.06$. With these conditions in place, we attempted to answer the following. First, what governs the time evolution of molecules in the supercritical state? Second, how does a dynamic structure correlate with a static structure? Third, what features appear when the DLS data of different molecules are scaled? Thus, in analyzing the data of time correlation functions of density inhomogeneity, we obtained several new insights into the time evolution of non-hydrogen-bonding fluids: the main contribution to the dynamics of density inhomogeneity; the universality of theoretical relations to nonpolar, dipolar, and nondipolar fluids; and the principle of the corresponding state from the perspective of dynamics measurements.

II. Experimental Section

The DLS instrument used in the present study has been described elsewhere.^{18,19} The light source was an argon-ion laser operating at a single line of 488 nm at a power of 100 mW. The scattering light was collected by an optical fiber that was attached to a goniometer and was detected with a photomultiplier tube in a photon-counting method. The counted photons were processed via a digital multiple- τ photon correlator (ALV 5000E). The laser, optics, goniometer, and detector were aligned with each other carefully, to an accuracy of ± 5 μ m, using a calibrated disk. A sufficient quality of data was able to be collected when the scattering angles were 20°–150°.

The optical cell for light scattering in a high-pressure condition has been described elsewhere.^{18,19} The cell was a Pyrex cylinder with a special smooth surface. The pressure and temperature of the fluid were adjusted by an injector and by circulating water, respectively. To maintain a homogeneous temperature, a heat insulator enclosed the assemblies that were attached to the cell. Fluctuations of pressure and temperature

during measurement were carefully adjusted to within a deviation of $\pm 0.03\%$.

In DLS experiments, a light-intensity auto-correlation function is measured by a digital photon correlator. This function, $g^{(2)}(t)$, is described by the use of an electric-field auto-correlation function $g^{(1)}(t)$ as follows:^{6,7}

$$g^{(2)}(t) = 1 + \beta |g^{(1)}(t)|^2 \quad (1)$$

where β is the coherence factor. By taking the square root of the quantity $g^{(2)}(t) - 1$, the value of $g^{(1)}(t)$ is obtained. In the case of neat fluids that consist of small molecules, the time profile of the electric-field correlation function is characterized by the dynamics of density fluctuation; this fluctuation is caused by the thermal fluctuation of a dielectric medium via diffusive and/or Brownian motion of molecules.^{6–8} In the present study, all data are measured at the scattering vector of $k = |\mathbf{k}| = 4\pi n \sin(\theta/2)/\lambda \cong 1.0 \times 10^{-2}$ nm⁻¹, whose scale corresponds to a mesoscopic region in real space. As a result, the electric-field correlation function here is ascribed to the time correlation of density fluctuation, and indicates time evolution in a mesoscopic volume, where numerous molecules are inhomogeneously dispersed.

We measured the time correlation functions of the density fluctuations of supercritical xenon, CHF₃, C₂H₄, and CO₂, whose critical constants are listed in Table 1. The data were collected in the density range of $0.4 \leq \rho_r \leq 1.6$ at four isotherms: $T_r = 1.01, 1.02, 1.04, \text{ and } 1.06$. Below room temperature, measurements were made carefully by flowing dried nitrogen gas (N₂) around the cell, to prevent condensation in the atmosphere. The chemical purity was commercially guaranteed to be >99.99%, and the fluid was filtrated with a polytetrafluoroethylene (PTFE) membrane filter with 0.1- μ m pores to increase the fluids’ optical purity.

III. Results

Figure 1 shows a typical example of the data obtained: the time correlation functions of the density fluctuation of supercritical xenon at $T_r = 1.01$. As shown, the functions decay to the baseline within a few microseconds. The symbols and solid lines indicate the experimental data and the fitting function of the single-exponential function, respectively. That is, all time correlation functions measured in the present study were well-analyzed by a single-exponential function, whose decay was responsible for the dynamics characterized by hydrodynamic theory.^{15,16} Thus, we obtain the correlation times (τ) from the time correlation functions of density fluctuation in the form of $\exp(-t/\tau)$ in all thermodynamic states and all molecules.

Using the measured time correlation functions, all correlation times were obtained for the four fluids, as listed in Tables 2–5. Note that these times were obtained at the scattering vectors, k

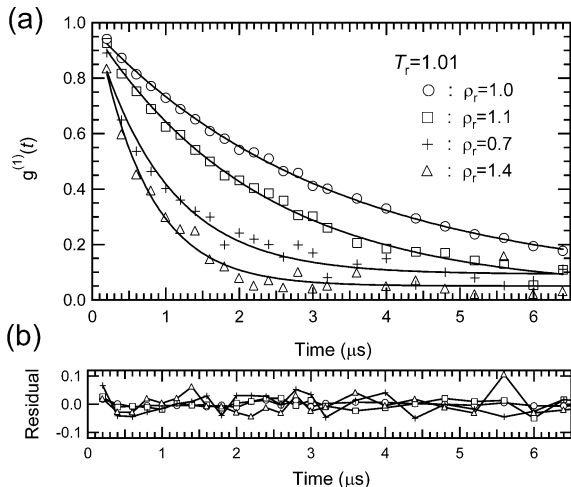


Figure 1. (a) Correlation functions of density fluctuation, indicating time evolution of Xe molecules inhomogeneously dispersing at the scattering angle of 42.5° and reduced temperature of $T_r = T/T_c = 1.01$. Solid symbols and lines denote experimental data and fitting curves with single-exponential functions, respectively. (b) Residuals between correlation functions and single-exponential functions.

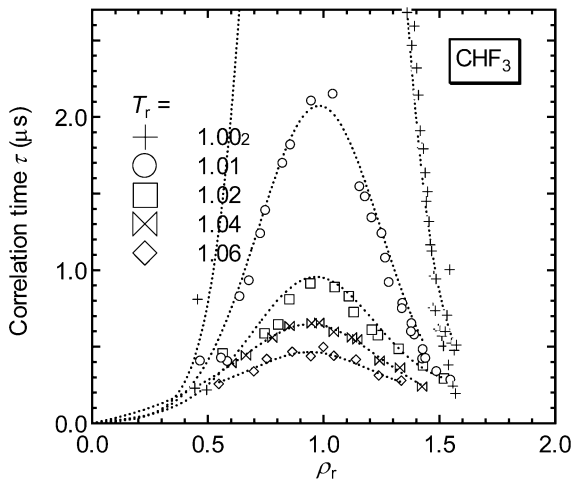


Figure 2. Correlation time of density fluctuation of supercritical CHF_3 , as a function of density at five isotherms.

$= 4\pi n \sin(\theta/2)/\lambda$, whose values are obtained from our measurements.³¹ That is, we measured the refractive indices, n , of four fluids at each density and temperature, and the scattering vectors are calibrated by the refractive indices. As a typical example of the data in the tables, the correlation times of supercritical CHF_3 are shown in Figure 2 as the density dependences at several temperatures. The temperature and density drastically change the values of the correlation times, which grow as the thermodynamic states approach the critical point. Note that the value of the correlation time becomes considerable at $\rho_r \approx 1.0$ and $T_r \approx 1.0$, and it diverges from there. That is, the time evolution of the density fluctuation becomes slower in the vicinity of $\rho_r = 1.0$ and $T_r = 1.0$. This observation corresponds to the “critical slowing down” observed in the time domain.

Figure 3 shows the correlation times of all of the measured fluids at the four isotherms. The differences in the values of these fluids are manifest at all measured temperatures. The correlation time of xenon is significantly greater than those of the other three fluids. Figure 4a shows the temperature dependences of the τ values of the four fluids measured at $\rho_r = 1.0$. All the values decline as the temperature moves away from the

TABLE 2: Correlation Times of Supercritical Xenon at Four Isotherms

P^a (MPa)	ρ (g/cm ³)	ρ_r	τ^b (μs)	$k^{c,d}$ (10^7 m^{-1})
$T_r = 1.01$				
5.81	0.653	0.594	0.645	1.028
6.00	0.764	0.695	0.859	1.044
6.10	0.876	0.796	1.94	1.060
6.14	0.978	0.889	3.51	1.075
6.18	1.096	0.997	3.42	1.092
6.22	1.210	1.10	2.27	1.108
6.27	1.307	1.19	2.02	1.122
6.62	1.529	1.39	0.492	1.155
6.66	1.545	1.40	0.717	1.157
$T_r = 1.02$				
6.10	0.693	0.630	0.550	1.034
6.30	0.817	0.742	0.857	1.052
6.42	0.936	0.851	1.29	1.069
6.51	1.062	0.965	1.96	1.087
6.54	1.107	1.01	1.99	1.094
6.59	1.178	1.07	1.81	1.104
6.71	1.318	1.20	1.13	1.124
6.87	1.418	1.29	0.708	1.138
$T_r = 1.04$				
6.92	0.885	0.805	0.684	1.062
7.09	0.996	0.905	0.853	1.078
7.17	1.060	0.964	1.04	1.087
7.23	1.103	1.00	0.837	1.093
7.24	1.110	1.01	1.00	1.094
7.39	1.208	1.10	0.870	1.108
7.52	1.280	1.16	0.743	1.118
$T_r = 1.06$				
7.41	0.866	0.787	0.722	1.059
7.66	0.977	0.888	0.793	1.075
7.85	1.063	0.967	0.807	1.087
7.90	1.086	0.987	0.664	1.091
8.09	1.169	1.06	0.704	1.102
8.12	1.185	1.08	0.601	1.105

^a Uncertainties of pressure during a measurement were <0.01 MPa.

^b Uncertainties of correlation times were in the range of 0.02 – $0.1 \mu\text{s}$.

^c The scattering vector, $k = 4\pi n \sin(\theta/2)/\lambda$, at each thermodynamic state were obtained from our data, which are the refractive indices (n) of supercritical xenon measured under the same experimental conditions as the present DLS measurements (ref 31). ^d Uncertainties of scattering vector, which is induced by uncertainties of refractive indices, were $<1\%$.

critical temperature. The data show another feature: the τ values are dependent on the samples. To compare the differences among dynamic structures, depending on the molecules, we obtained the ratio of correlation times at $\rho_r = 1.0$ and $T_r = 1.02$ (i.e., $\tau(\text{CHF}_3):\tau(\text{C}_2\text{H}_4):\tau(\text{CO}_2):\tau(\text{Xe}) = 1.5:1.0:1.5:2.5$). The greater ratio of correlation time indicates the slower dynamics of density fluctuation. Thus, the supercritical xenon shows the slowest time evolution of density fluctuation among the four fluids, whereas the supercritical C_2H_4 shows the fastest. On the other hand, the dynamics of CHF_3 are similar to those of CO_2 . Let us confirm the difference in correlation time between these two fluids, from the point of view of molecular velocity and viscosity. This is because the value of the correlation time is governed by the dynamics of density fluctuation, characterized by the Brownian motion of molecules in viscous fluid. For examples, the ratio of velocity that was approximated by the kinetic energy at the measured temperatures was $1/v(\text{CHF}_3):1/v(\text{C}_2\text{H}_4):1/v(\text{CO}_2):1/v(\text{Xe}) = 1.6:1.0:1.3:2.2$, and the ratio of viscosity at $\rho_r = 1$ and $T_r = 1.02$ was $\eta(\text{CHF}_3):\eta(\text{C}_2\text{H}_4):\eta(\text{CO}_2):\eta(\text{Xe}) = 1.5:1.0:1.5:2.5$.^{32–35} Consequently, the ratio of correlation times among these four fluids is similar to the ratios of velocity and viscosity. The latter agrees particularly well with the ratio of correlation time.

TABLE 3: Correlation Times of Supercritical CHF₃ at Five Isotherms

P^a (MPa)	ρ (g/cm ³)	ρ_r	τ^b (μ s)	$k^{c,d}$ (10 ⁷ m ⁻¹)	P^a (MPa)	ρ (g/cm ³)	ρ_r	τ^b (μ s)	$k^{c,d}$ (10 ⁷ m ⁻¹)
$T_r = 1.002$									
4.35	0.233	0.444	0.229	1.023	5.29	0.761	1.45	1.51	1.115
4.39	0.239	0.455	0.808	1.026	5.31	0.764	1.46	1.32	1.115
4.95	0.640	1.22	4.17	1.094	5.33	0.767	1.46	1.16	1.116
5.03	0.699	1.33	3.49	1.104	5.35	0.770	1.47	1.12	1.116
5.07	0.714	1.36	2.68	1.107	5.38	0.773	1.47	0.752	1.117
5.09	0.720	1.37	2.72	1.108	5.39	0.775	1.48	0.959	1.117
5.11	0.725	1.38	2.47	1.109	5.42	0.778	1.48	0.733	1.118
5.14	0.731	1.39	2.59	1.110	5.43	0.780	1.49	0.942	1.118
5.16	0.736	1.40	2.32	1.110	5.59	0.797	1.52	0.503	1.121
5.18	0.740	1.41	2.14	1.111	5.63	0.801	1.53	0.598	1.121
5.19	0.744	1.42	1.91	1.112	5.68	0.805	1.53	0.705	1.122
5.22	0.748	1.42	1.80	1.112	5.71	0.808	1.54	0.380	1.123
5.23	0.751	1.43	1.79	1.113	5.80	0.815	1.55	0.522	1.124
5.26	0.755	1.44	1.63	1.114	5.88	0.821	1.56	0.474	1.125
5.27	0.758	1.44	1.45	1.114	5.95	0.826	1.57	0.510	1.126
$T_r = 1.01$									
4.56	0.246	0.469	0.403	1.028	5.38	0.666	1.27	1.07	1.099
4.98	0.336	0.640	0.823	1.043	5.40	0.674	1.28	0.916	1.100
5.03	0.357	0.680	0.928	1.046	5.49	0.704	1.34	0.745	1.105
5.09	0.383	0.730	1.23	1.051	5.49	0.705	1.34	0.780	1.105
5.11	0.394	0.750	1.39	1.053	5.58	0.725	1.38	0.595	1.109
5.17	0.433	0.825	1.70	1.059	5.59	0.726	1.38	0.647	1.109
5.19	0.451	0.859	1.81	1.062	5.62	0.732	1.39	0.574	1.110
5.22	0.498	0.949	2.10	1.070	5.73	0.750	1.43	0.416	1.113
5.25	0.547	1.04	2.15	1.078	5.74	0.751	1.43	0.478	1.113
5.29	0.608	1.12	1.54	1.089	5.78	0.757	1.44	0.421	1.114
5.30	0.620	1.18	1.48	1.091	6.00	0.782	1.49	0.334	1.118
5.32	0.635	1.21	1.34	1.093	6.39	0.814	1.55	0.279	1.124
5.36	0.658	1.25	1.24	1.097					
$T_r = 1.02$									
5.02	0.296	0.564	0.454	1.036	5.70	0.593	1.43	0.377	1.113
5.36	0.391	0.851	0.808	1.062	5.79	0.634	1.52	0.291	1.121
5.43	0.422	0.943	0.911	1.070	5.83	0.648	0.745	0.586	1.052
5.48	0.447	1.05	0.889	1.079	6.01	0.695	0.804	0.645	1.057
5.56	0.495	1.13	0.724	1.086	6.37	0.750	1.11	0.828	1.084
5.63	0.550	1.23	0.574	1.096	6.91	0.798	1.21	0.609	1.093
5.68	0.582	1.32	0.485	1.103					
$T_r = 1.04$									
5.52	0.317	0.604	0.389	1.040	6.41	0.549	1.05	0.593	1.079
5.69	0.350	0.667	0.440	1.045	6.56	0.590	1.12	0.557	1.086
5.95	0.410	0.781	0.555	1.055	6.61	0.602	1.15	0.544	1.088
6.09	0.449	0.855	0.631	1.062	6.85	0.653	1.24	0.405	1.096
6.25	0.499	0.950	0.649	1.070	7.16	0.699	1.33	0.359	1.104
6.30	0.516	0.983	0.651	1.073	7.66	0.749	1.43	0.235	1.113
$T_r = 1.06$									
5.70	0.288	0.549	0.252	1.035	7.08	0.525	1.00	0.494	1.075
6.26	0.368	0.700	0.334	1.048	7.20	0.549	1.04	0.437	1.079
6.43	0.397	0.756	0.416	1.053	7.49	0.599	1.14	0.412	1.087
6.73	0.455	0.867	0.463	1.063	7.86	0.651	1.24	0.308	1.096
6.94	0.497	0.947	0.434	1.070	8.35	0.702	1.33	0.275	1.105

^a Uncertainties of pressure during a measurement were <0.01 MPa. ^b Uncertainties of correlation times were in the range of 0.02–0.1 μ s. ^c The scattering vector, $k = 4\pi n \sin(\theta/2)/\lambda$, at each thermodynamic state were obtained from our data, which are the refractive indices (n) of supercritical CHF₃ measured under the same experimental conditions as the present DLS measurements (ref 31). ^d Uncertainties of scattering vector, which are induced by uncertainties of refractive indices, were <1%.

IV. Discussion

IV.A. Contribution of Molecules in Non-hydrogen-bonding Fluids to Time Evolution at Supercritical Regions. We discuss the relationships among correlation time, temperature, and viscosity to investigate the contributions of non-hydrogen-bonding fluids to density fluctuation dynamics. According to the Kawasaki theory and the Landau–Placzek theory, correlation time is described as follows:^{36–38}

$$\frac{1}{\tau k^2} = D_T = \frac{\lambda}{\rho C_p} = \frac{k_B T}{6\pi\eta\xi} \frac{\lambda}{\lambda_c} \quad (2)$$

where τ is correlation time, k the scattering vector, D_T the

thermal diffusivity, λ the thermal conductivity, ρ the density, C_p the specific heat capacity at constant pressure, k_B the Boltzmann constant, T the temperature, η the viscosity, ξ the correlation length, and λ_c the critical part of thermal conductivity. These theoretical relations were verified by experiments on supercritical CO₂ in the thermodynamic state at a density of $\rho_r = 1.0$ very near the critical temperature. We suppose here that this relationship would be established in the present thermodynamic states of the fluids used (vide infra). Also in this section, we discuss the dynamics of density fluctuation. In eq 2, the correlation time (τ) and correlation length (ξ) are involved on the left-hand and right-hand sides, respectively. As described in section III, τ showed significant molecular dependence. On

TABLE 4: Correlation Times of Supercritical C₂H₄ at Four Isotherms

P^a (MPa)	ρ (g/cm ³)	ρ_r	τ^b (μ s)	$k^{c,d}$ (10 ⁷ m ⁻¹)
$T_r = 1.01$				
5.06	0.128	0.596	0.332	1.022
5.20	0.146	0.682	0.413	1.035
5.29	0.170	0.794	0.534	1.052
5.32	0.184	0.857	0.700	1.061
5.35	0.203	0.950	1.37	1.075
5.37	0.219	1.02	1.34	1.086
5.39	0.232	1.08	1.23	1.095
5.41	0.242	1.13	1.09	1.102
5.44	0.253	1.18	0.816	1.110
5.52	0.270	1.26	0.449	1.122
5.64	0.285	1.33	0.377	1.132
5.76	0.294	1.37	0.288	1.139
$T_r = 1.02$				
5.07	0.115	0.536	0.380	1.013
5.37	0.141	0.658	0.482	1.032
5.44	0.152	0.707	0.542	1.039
5.59	0.181	0.846	0.688	1.060
5.64	0.196	0.915	0.652	1.070
5.70	0.219	1.02	0.748	1.086
5.78	0.240	1.12	0.723	1.101
5.85	0.254	1.19	0.610	1.110
6.05	0.278	1.30	0.453	1.127
6.18	0.287	1.34	0.363	1.134
$T_r = 1.04$				
5.52	0.123	0.573	0.218	1.019
5.90	0.154	0.719	0.275	1.041
6.00	0.165	0.771	0.325	1.048
6.11	0.179	0.836	0.386	1.058
6.22	0.195	0.910	0.465	1.069
6.30	0.208	0.969	0.500	1.078
6.41	0.223	1.04	0.488	1.089
6.49	0.234	1.09	0.382	1.096
6.60	0.246	1.15	0.352	1.105
6.69	0.255	1.19	0.330	1.111
6.77	0.262	1.22	0.364	1.116
6.88	0.269	1.26	0.271	1.121
$T_r = 1.06$				
6.08	0.136	0.635	0.220	1.028
6.37	0.156	0.729	0.287	1.042
6.65	0.180	0.840	0.331	1.059
6.77	0.191	0.892	0.306	1.066
6.86	0.200	0.934	0.326	1.073
6.97	0.211	0.984	0.336	1.080
7.15	0.227	1.06	0.319	1.092
7.44	0.248	1.16	0.286	1.106
7.63	0.259	1.21	0.203	1.114

^a Uncertainties of pressure during a measurement were <0.01 MPa.

^b Uncertainties of correlation times were in the range of 0.02–0.1 μ s.

^c The scattering vectors, $k = 4\pi n \sin(\theta/2)/\lambda$, at each thermodynamic state were obtained using our data, which are the refractive indices (n) of supercritical C₂H₄ measured under the same experimental conditions as the present DLS measurements (ref 31). ^d Uncertainties of scattering vector, which are induced by uncertainties of refractive indices, were <1%.

the other hand, the ξ value obtained from SAXS measurements was reported to be almost independent of the molecules³⁹ used in the present study. Under these situations, it is understood that the molecular dependence of τ results from the values of T , η , and λ/λ_c in eq 2.

Here, a portion of eq 2 is rewritten as follows:

$$\left(\frac{k_B T}{6\pi\eta\xi}\right)\frac{\lambda}{\lambda_c} = \frac{k_B T}{6\pi\eta R_H} \quad (3)$$

where R_H corresponds to the average hydrodynamic radius of clusters in supercritical fluids. Using eqs 2 and 3, we investigated

TABLE 5: Correlation Times of Supercritical CO₂ at Three Isotherms

P^a (MPa)	ρ (g/cm ³)	ρ_r	τ^b (μ s)	$k^{c,d}$ (10 ⁷ m ⁻¹)
$T_r = 1.01$				
7.42	0.274	0.587	0.393	1.030
7.64	0.320	0.684	0.542	1.041
7.74	0.353	0.754	0.711	1.048
7.81	0.389	0.831	1.47	1.056
7.84	0.411	0.879	1.90	1.061
7.87	0.439	0.938	1.91	1.068
7.88	0.449	0.960	1.92	1.070
7.90	0.469	1.00	1.71	1.075
7.92	0.488	1.04	1.44	1.079
7.94	0.505	1.08	1.32	1.083
7.98	0.532	1.14	0.984	1.089
8.01	0.548	1.17	0.797	1.093
8.05	0.564	1.21	0.617	1.096
8.10	0.582	1.24	0.529	1.100
$T_r = 1.02$				
7.11	0.218	0.466	0.347	1.018
8.06	0.337	0.720	0.618	1.045
8.27	0.401	0.857	0.774	1.059
8.36	0.439	0.938	0.896	1.068
8.42	0.468	1.00	0.949	1.074
8.47	0.486	1.04	0.879	1.079
8.54	0.514	1.10	0.753	1.085
8.60	0.533	1.14	0.690	1.089
8.80	0.579	1.24	0.520	1.100
$T_r = 1.04$				
8.60	0.313	0.669	0.452	1.039
8.71	0.327	0.700	0.470	1.042
8.79	0.339	0.724	0.500	1.045
8.90	0.356	0.761	0.536	1.049
8.94	0.362	0.773	0.572	1.050
9.00	0.372	0.796	0.580	1.053
9.08	0.386	0.825	0.596	1.056
9.14	0.399	0.854	0.596	1.059
9.21	0.413	0.884	0.634	1.062
9.29	0.428	0.916	0.587	1.065

^a Uncertainties of pressure during a measurement were <0.01 MPa.

^b Uncertainties of correlation times were in the range of 0.02–0.1 μ s.

^c The scattering vector, $k = 4\pi n \sin(\theta/2)/\lambda$, at each thermodynamic state were obtained from our data, which are the refractive indices (n) of supercritical CO₂ measured under the same experimental conditions to present DLS measurements (ref 31). ^d Uncertainties of scattering vector, which is induced by uncertainties of refractive indices, were <1%.

the fluid dependence of τ using the values of viscosity, temperature, and density. That is, we obtained a static parameter (R_H) and considered what governs the time evolution of molecules of non-hydrogen-bonding fluids in the supercritical states. Figure 4b shows the R_H values of four fluids at a density of $\rho_r = 1.0$, as a function of temperature. The R_H values become almost the same in all four fluids at all reduced temperatures and densities in the present ranges. This situation is consistent with the static fluctuation; that is, the correlation length obtained from the SAXS measurements is mostly independent of the molecules³⁹ used in the present study at all reduced temperatures and densities. From these results, it is elucidated that, although the time evolution of density fluctuation shows significant molecular dependence, such dependence disappears by scaling the dynamic parameter to the static parameter through the use of viscosity. Thus, the present experimental results and analysis showed that viscosity is the principal contributor to the molecular dependence of the time evolution of density fluctuation. Such a situation is established in non-hydrogen-bonding fluids of nonpolar, dipolar, and nondipolar molecules at the supercritical states.

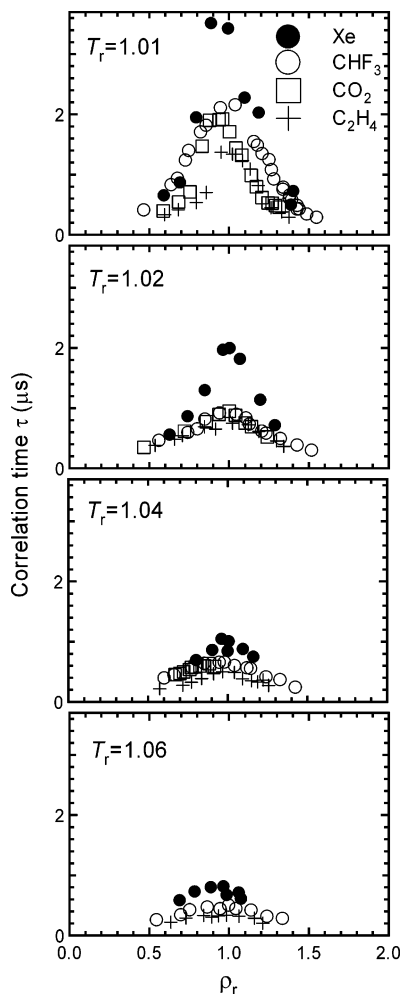


Figure 3. All correlation times measured in the supercritical regions; the data show the times of supercritical xenon, CHF₃, CO₂, and C₂H₄, as a function of the density.

IV.B. The Principle of Corresponding State Observed from Time-Domain Measurements and the Kawasaki Theory and Landau–Placzek Theory. In this section, we introduce another parameter—the reduced hydrodynamic radius, R_H' —and discuss the theoretical relation of eq 2. Since a hydrodynamic radius is reduced by dividing R_H by the van der Waals radius, the term R_H' is a dimensionless parameter. Figure 4c shows the R_H' values of four fluids, as a function of temperature. It can be observed that these values agree well among the four fluids. According to the principle of corresponding state, it has been known that the universality among different fluids appears around the critical point, and that the property of molecules disappears there by reducing the physical value to a dimensionless parameter, despite the significant differences of molecules.¹ Note that the observed experimental results—the dimensionless parameter R_H' in Figure 4c—shows such a feature. As another specific feature, the result in Figure 4c is very similar to that observed in previous observations of the principle of corresponding state.^{39,40} In that paper, reduced correlation lengths were in good agreement among supercritical CO₂, CHF₃, and C₂H₄, and the observed principle of corresponding of state was confirmed theoretically by the van der Waals theory and thermodynamic calculation.⁴⁰ Based on the present and previous results, we considered that the agreement of the dimensionless parameters among the different fluids shown in Figure 4c is responsible for the principle of corresponding state.

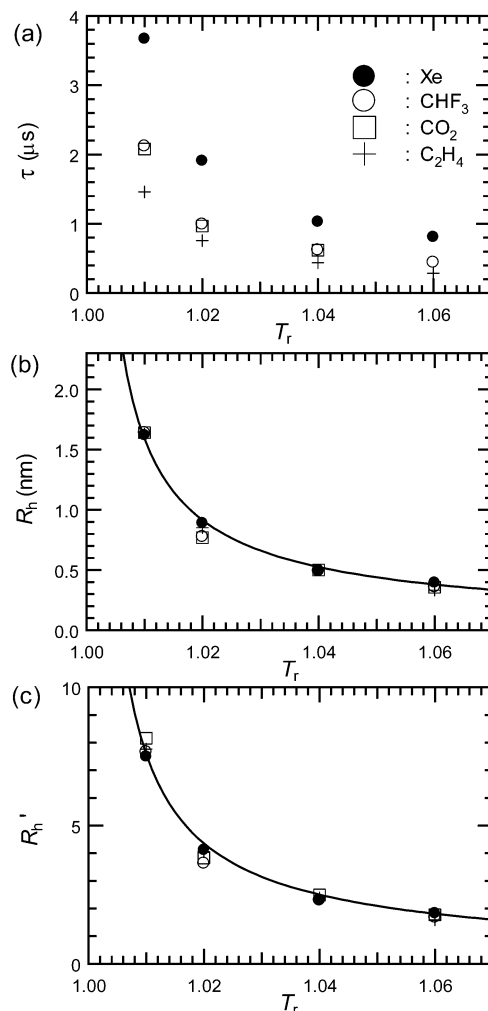


Figure 4. Temperature dependences of (a) correlation times, (b) hydrodynamic radii of clusters, and (c) reduced hydrodynamic radii of clusters of supercritical xenon, CHF₃, CO₂, and C₂H₄; the data were obtained at a reduced density of $\rho_r = \rho/\rho_c = 1.0$.

To the best of our knowledge, this is the first time that this universality has been observed through time-domain measurements.

The data shown in Figure 4c are obtained from the use of eq 2, based on the Kawasaki theory and the Landau–Placzek theory. The principle of corresponding state is also obtained from eq 2. Although the theoretical relation in eq 2 was confirmed by experiments in two previous reports,^{36,37} the experimental conditions in those studies were very restricted: the only fluid was supercritical CO₂, and the thermodynamic state was very close to the critical temperature, such as $T_r = 1.0001$. As a result, it has been unclear whether the theoretical relation of eq 2 has been established for specific molecules and thermodynamic states (vide supra). Let us discuss this briefly, using our experimental results. In the present study, the principle of corresponding state is observed for four polar, nonpolar, and non-dipolar fluids: supercritical CHF₃, xenon, CO₂, and C₂H₄. This observation is obtained by measuring DLS and using eq 2, and it is obtained at temperatures relatively far from the critical temperature, such as $T_r = 1.02$ – 1.06 . Supercritical CO₂, C₂H₄, and CHF₃ are studied in the present DLS and previous SAXS studies at temperatures relatively far from the critical temperature, such as $T_r = 1.02$ – 1.06 . Both the agreement of experimental results and conditions between these studies allow us to understand that the theoretical relation of

eq 2 characterizes the principle of corresponding state and can be applied to various supercritical fluids and thermodynamic states. That is, eq 2 is applied to not only supercritical CO₂ but also nonpolar, dipolar, and non-dipolar fluids, and the thermodynamic state is expanded to one relatively far from the critical temperature. This means that the Kawasaki theory and the Landau–Placzek theory seem to be universally established in various non-hydrogen-bonding fluids in the supercritical regions.

IV.C. Average Cluster Size in Supercritical Fluids, as a Function of Temperature. As described in section IV.A, the value of R_H is the hydrodynamic radius—the average radius of clusters in the neat supercritical fluids. On the other hand, the value of R_H' was the cluster radius normalized by the molecular radius and corresponded to the cluster radius, which is a dimensionless parameter. This dimensionless parameter is the cluster size divided by the molecular size; therefore, the resulting value, R_H' , tells us how many molecules are in the cluster. That is, the larger the R_H' value, the greater the number of molecules. Figure 4c shows the R_H' of four fluids, as a function of temperature. The R_H' values increase as the temperature approaches T_c . This means that the clusters grow as the temperature approaches T_c . In recent theoretical research, clustering in a neat supercritical fluid was investigated by changing the intermolecular potentials.⁴¹ In that study, it was revealed that the strength of an intermolecular potential and the temperature have important roles in determining the degree of clustering in supercritical states. In the current study, as temperature approaches T_c , the experimental result shows that the cluster grows. These theoretical and experimental results show that the attractive intermolecular interactions for clusterization become gradually dominant as the temperature approaches T_c .

Next, we compare the values obtained in the present study to the values obtained in the previous studies; i.e., (i) the R_H value in the present study; (ii) the R_H value calculated from eq 2, using the heat capacity,⁴² thermal conductivity,^{43,44} density, and viscosity;³³ (iii) the correlation length ξ , obtained from the SAXS measurement;³⁹ and (iv) the ξ value from the correlation time τ obtained in the present DLS measurement. The correlation length is defined as follows:¹

$$g(r) - 1 = k_B T \kappa_T \left[\frac{\exp\left(-\frac{r}{\xi}\right)}{4\pi\xi^2 r} \right] \quad (4)$$

where $g(r)$ is a two-body correlation function and κ_T is the isothermal compressibility. Figure 5a shows these four values for supercritical CO₂, as a function of temperature, at $\rho_r = 1.0$. Note the good agreement among these four values, whose data are obtained from different experiments and calculations, as mentioned previously. Based on this coincidence, it was also verified from another approach that the theoretical expression of eq 2 given by the Kawasaki theory and the Landau–Placzek theory is well-established.

IV.D. Density Inhomogeneity Obtained from Time-Domain Measurements. The long-range density inhomogeneity has been well-characterized by the density fluctuation. The density fluctuation is formulated by the number-density inhomogeneity as follows:¹

$$\frac{\langle(\Delta N)^2\rangle}{\langle N\rangle} = \frac{\langle(N - \langle N\rangle)^2\rangle}{N} = \frac{I(0)}{Z^2\langle N\rangle} = \left(\frac{N}{V}\right) \kappa_T k_B T \quad (5)$$

where N is the number of molecules in volume V , $\langle N \rangle$ is

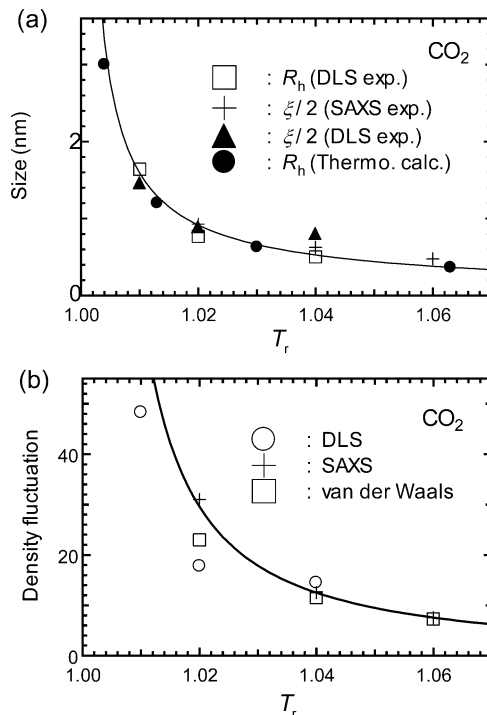


Figure 5. (a) Comparison among the hydrodynamic radius R_H obtained from the present study, R_H from the calculation by the use of transport coefficients, and the correlation lengths ξ obtained from the previous small-angle X-ray scattering (SAXS) and the present DLS measurements at the same thermodynamic state of supercritical CO₂. (b) Comparison among density fluctuations of supercritical CO₂ obtained from the correlation time in the present study, a set of SAXS measurements and isothermal compressibility, and the van der Waals equation.

ensemble-averaged value, $I(0)$ the scattering intensity at scattering vector $k = 0$, Z the number of electrons of a molecule, and κ_T the isothermal compressibility. According to eq 5, the value of density fluctuation is obtained from either or both of two methods: measurement of scattered intensity at $k = 0$ and measurement of the value of κ_T . The former gives only a relative value of density fluctuation, because of the experimental difficulty of measuring the absolute scattering intensity at $k = 0$, whereas the latter offers an absolute value by measuring both κ_T and density or by differentiating the state equation with $P-V-\rho-T$ relations. Such κ_T is formulated by eq 6:³⁷

$$\kappa_T = \frac{\xi^2}{R^2 \rho_n k_B T} \quad (6)$$

where R is the direct correlation length³⁷ and ρ_n is the number density. By substituting eqs 2 and 6 into eq 5, the following equation is obtained:

$$\frac{\langle(\Delta N)^2\rangle}{\langle N\rangle} = \left(\frac{\tau k^2 k_B T \lambda}{6\pi\eta R \lambda_c} \right)^2 \quad (7)$$

Thus, we are able to estimate the absolute value of density fluctuation using the correlation time of the DLS measurement and the transport coefficients.^{33,44} We then compared the density fluctuations of the present absolute value with the values obtained by the other methods. Figure 5b shows the density fluctuations along the critical isochore of supercritical CO₂, as a function of temperature; the open circle, cross, and square symbols represent the data given by the present correlation time, the SAXS measurement, and the state equation of van der

Waals,⁴⁰ respectively. The solid line is evaluated using the critical index of isothermal compressibility.⁴⁵ Figure 5b shows three significant points. First, the present report is the first to estimate the value of density fluctuation using time-domain data. Second, the value obtained in this study agrees with the other density fluctuations. Third, the value of density fluctuation was also estimated from eq 2. Thus, it was verified from the other approach that the theoretical expression of eq 2 given by the Kawasaki theory and the Landau–Placzek theory is well-established.

Finally, let us mention the universality of λ/λ_c , which is observed in the present result. According to eq 3, the value of λ/λ_c is expressed by the equation $\xi = R_H \lambda/\lambda_c$, whose ratio λ/λ_c was reported to be 2 for the supercritical CO₂.^{43,44} As shown in Figure 4, the values of R_H are the same among the four fluids. On the other hand, the values of ξ are in good agreement in the supercritical CHF₃, CO₂, and C₂H₄ from the previous study of SAXS measurements.³⁹ Under these conditions, the value of λ/λ_c is not dependent on the type of molecules. That is, the universality of λ/λ_c can be suggested in these three fluids. This observation of the universality of λ/λ_c will be important information for discussions of phenomena around the gas–liquid critical point. This is because the λ/λ_c is essential for obtaining the density fluctuation from the time-domain experiments, and, thus, for obtaining an absolute value for density fluctuation.

V. Concluding Remarks

The dynamics of fluctuations in the density of supercritical CHF₃, C₂H₄, CO₂, and xenon were studied by observing the time evolution of molecules in supercritical states from measurements of dynamic light scattering. The obtained time correlation functions were analyzed on the basis of the Kawasaki theory and the Landau–Placzek theory. The molecular dependences of dynamic and static fluctuations were studied under conditions relatively far from the gas–liquid critical points of these four fluids. The following conclusions were obtained:

(1) The time evolution of molecules that have been inhomogeneously dispersed is characterized by a single-exponential function in all thermodynamic states and all fluids within the present ranges of experimental conditions. The “critical slowing down” was observed for all fluids by the time-domain measurements, and it became more noteworthy as the thermodynamic states approached the critical point.

(2) The correlation times of density fluctuation were not the same but were dependent significantly on the type of molecules. By scaling the obtained dynamic parameters to the static parameters, the molecular dependence disappeared completely. It was elucidated that viscosity is the principal contribution governing the molecular differences in time evolutions among nonpolar, dipolar, and non-dipolar fluids that have no hydrogen bonding.

(3) The possibility of whether the theoretical relations given by the Kawasaki theory and the Landau–Placzek theory are applicable to certain molecules and thermodynamic states was investigated. These theorems were confirmed to be (i) applicable to polar, nonpolar, and non-dipolar fluids that have no hydrogen bonding and (ii) extensible to temperatures relatively far from the critical temperature.

(4) The density fluctuation correlation lengths and the values of density fluctuations were estimated using time-domain data, and these estimates were evaluated by comparing those values with the long-range density inhomogeneities obtained from other experiments and/or calculations. The estimated values agreed consistently with values obtained from SAXS experiments, from

calculations by transport coefficient and from calculations of isothermal compressibility. In this estimation, it was also confirmed that the theoretical relation due to the Kawasaki theory and the Landau–Placzek theory is well-accomplished.

Acknowledgment. This work was partially supported by a Grant-in-Aid for Scientific Research from the Ministry of Education, Science, and Culture, Japan. K.S. wishes to thank the Collaboration Research Foundation for a grant for young researchers at the Graduate School of Science and Technology of Chiba University.

References and Notes

- (1) Stanley, H. E. *Introduction to Phase Transitions and Critical Phenomena*; Oxford University Press: New York, 1971.
- (2) Greer, S. C.; Moldover, M. R. *Annu. Rev. Phys. Chem.* **1981**, *32*, 233.
- (3) Sengers, J. V.; Sengers, J. M. H. L. *Annu. Rev. Phys. Chem.* **1986**, *37*, 189.
- (4) Kajimoto, O. *Chem. Rev.* **1999**, *99*, 355.
- (5) Tucker, S. C. *Chem. Rev.* **1999**, *99*, 391.
- (6) Berne, B. J.; Pecora, R. *Dynamic Light Scattering*; Wiley–Interscience: New York, 1976.
- (7) Chu, B. *Laser Light Scattering: Basic Principles and Practice*; Academic Press: Boston, 1991.
- (8) Mountain, R. D. *Rev. Mod. Phys.* **1966**, *38*, 205.
- (9) Lunacek, J. H.; Cannell, D. S. *Phys. Rev. Lett.* **1971**, *27*, 841.
- (10) Maccabee, B. S.; White, J. A. *Phys. Lett.* **1971**, *35A*, 187.
- (11) White, J. A.; Maccabee, B. S. *Phys. Rev. Lett.* **1971**, *26*, 1468.
- (12) Cannell, D. S. *Phys. Rev. A* **1975**, *12*, 225.
- (13) Swinney, H. L.; Henry, D. L. *Phys. Rev.* **1973**, *8*, 2586 and references therein.
- (14) Letaief, A.; Tufeu, R.; Garrabos, Y.; Neindre, B. L. *J. Chem. Phys.* **1986**, *84*, 921.
- (15) Kawasaki, K. *Ann. Phys.* **1970**, *61*, 1.
- (16) Kawasaki, K. *Phys. Rev. A* **1970**, *1*, 1750.
- (17) Landau, L.; Placzek, G. *Phys. Z. Sowjetunion* **1934**, *5*, 172.
- (18) Saitow, K.; Ochiai, H.; Kato, T.; Nishikawa, K. *J. Chem. Phys.* **2002**, *116*, 4985.
- (19) Saitow, K.; Kajiya, D.; Nishikawa, K. *J. Am. Chem. Soc.* **2004**, *126*, 422.
- (20) Saitow, K.; Otake, H.; Nakayama, H.; Ishii, K.; Nishikawa, K. *Chem. Phys. Lett.* **2003**, *368*,
- (21) Saitow, K.; Nakayama, H.; Ishii, K.; Nishikawa, K. *J. Phys. Chem. A* **2004**, *108*, 5770.
- (22) Saitow, K.; Ohtake, H.; Sarukura, N.; Nishikawa, K. *Chem. Phys. Lett.* **2001**, *341*, 86.
- (23) Edward, J. T. *J. Chem. Edu.* **1970**, *47*, 261.
- (24) Gilliam, O. R.; Edwards, H. D.; Gordy, W. *Phys. Rev.* **1954**, *75*, 1014.
- (25) Gy, C. G.; Gubbins, K. E.; Dagg, I. R.; Read, L. A. A. *Chem. Phys. Lett.* **1980**, *73*, 278.
- (26) Glaser, R.; Wu, Z.; Lewis, M. J. *Mol. Struct. (THEOCHEM)* **2000**, *556*, 131.
- (27) McCarty, R. D. *Corrections for the Thermophysical Properties of Xenon*; NIST: Boulder, CO, 1989.
- (28) Aizpiri, A. G.; Rey, J.; Davila, J.; Rubio, R. G.; Zollweg, J. A.; Streett, B. J. *Chem. Phys.* **1991**, *95*, 3351.
- (29) Smulkara, J.; Span, R.; Wanger, W. *J. Phys. Chem. Ref. Data* **2000**, *29*, 1053.
- (30) Span, R.; Wagner, W. *J. Phys. Chem. Ref. Data* **1996**, *25*, 1509–1596.
- (31) Kajiya, D.; Saitow, K.; Nishikawa, K. Manuscript in preparation.
- (32) Yokoyama, C.; Takahashi, M. *Int. J. Thermophys.* **1997**, *18*, 1369.
- (33) Iwasaki, H.; Takahashi, M. *J. Chem. Phys.* **1981**, *74*, 1930.
- (34) Iwasaki, H.; Takahashi, M. In *Proceedings of the 4th International Conference on High Pressure*, Kyoto, Japan, 1974, p 523.
- (35) Stumpt, H. J.; Collings, A. F.; Pings, C. J. *J. Chem. Phys.* **1974**, *60*, 3109.
- (36) Sengers, J. V.; Keyes, P. H. *Phys. Rev. Lett.* **1971**, *26*, 70 and references therein.
- (37) Maccabee, B. S.; White, J. A. *Phys. Rev. Lett.* **1971**, *27*, 495 and references therein.
- (38) The equation given by the Kawasaki theory and the Landau–Placzek theory was partially corrected and has been obtained as the expression of eq 2. Using eq 2, Maccabee and White obtained the new values of correlation length and thermal diffusivity of supercritical CO₂.

These corrected values were 2–5 times smaller than the previously reported values. This story was described in refs 36 and 37 and was re-examined in ref 13.

(39) Nishikawa, K.; Ochiai, H.; Saitow, K.; Morita, T. *Chem. Phys.* **2003**, 286, 421.

(40) Nishikawa, K.; Kusano, K.; Arai, A. A.; Morita, T. *J. Chem. Phys.* **2003**, 118, 1341.

(41) Egorov, S. A. *Chem. Phys. Lett.* **2002**, 354, 140.

(42) <http://webbook.nist.gov/chemistry/fluid>.

(43) Giglio, M.; Benedek, G. B. *Phys. Rev. Lett.* **1969**, 17, 1145.

(44) Neidre, B. L.; Garrabos, Y.; Tufeu, R. *Int. J. Thermophys.* **1991**, 12, 307.

(45) Vesovic, V.; Wakeham, W. A.; Olhowy, G. A.; Sengers, J. V.; Watson, J. T. R.; Millat, J. *J. Phys. Chem. Ref. Data* **1990**, 19, 763.